

UNSUPERVISED STEREO MATCHING NETWORK FOR VHR REMOTE SENSING IMAGES BASED ON ERROR PREDICTION

Liting Jiang^{1,2,3}, Yuming Xiang^{1,2,3}, Feng Wang^{1,2,3}, and Hongjian You^{1,2,3}

1. Aerospace Information Research Institute, Chinese Academy of Sciences

2. Key Laboratory of Technology in Geo-spatial Information Processing and Application System,
Chinese Academy of Sciences, Beijing, 100190, China

3. School of Electronic, Electrical and Communication Engineering,
University of Chinese Academy of Sciences, Beijing, 101408, China

ABSTRACT

Stereo matching in remote sensing has recently garnered increased attention, primarily focusing on supervised learning. However, datasets with ground truth generated by expensive airborne Lidar exhibit limited quantity and diversity, constraining the effectiveness of supervised networks. In contrast, unsupervised learning methods can leverage the increasing availability of very-high-resolution (VHR) remote sensing images, offering considerable potential in the realm of stereo matching. Motivated by this intuition, we propose a novel unsupervised stereo matching network for VHR remote sensing images. A light-weight module to bridge confidence with predicted error is introduced to refine the core model. Robust unsupervised losses are formulated to enhance network convergence. The experimental results on US3D and WHU-Stereo datasets demonstrate that the proposed network achieves superior accuracy compared to other unsupervised networks and exhibits better generalization capabilities than supervised models. Our code will be available at <https://github.com/Elenairene/CBEM>.

Index Terms— Stereo matching, unsupervised learning, uncertainty, disparity estimation

1. INTRODUCTION

As Earth observation and computer vision technologies rapidly advance, 3D reconstruction has gained increasing attention in remote sensing. Stereo matching, a crucial step in 3D reconstruction, generates dense pixel-by-pixel matches, yielding disparity maps that enable height information extraction. The application of 3D reconstruction in remote sensing offers a novel perspective for observation and analysis of the Earth's surface, emerging as a prominent research topic.

Traditional stereo matching methods such as Semi-Global-Matching (SGM) algorithm [1] has been widely used. But deep learning methods have achieved better performance recently and are experiencing a significant development. GC-Net [2] first adopted 3D convolutions to construct cost volume. PSMNet [3] introduced spatial pyramid pooling to enlarge the receptive fields and employed stacked hour-glass module. Current state-of-the-art methods mostly use multi-feature 4D cost volume which burdens memory a lot

such as GANet [4] and CSPN [5]. To alleviate this problem, CFNet [6] employs uncertainty estimation to adjust disparity search range which reduces memory consumption. Bidir-EPNet [7] is designed as a specialized pyramid stereo matching network for VHR images. While datasets commonly used in supervised learning methods suffer from lack of diversity, unsupervised methods are unconstrained by availability of ground truth. UnFlow [8] proposed efficient unsupervised loss to train FlowNet without ground truth. PASM [9] applied attention mechanism to stereo matching task. Some unsupervised methods [10] have been applied in automatic driving and have promising future prospects. T. Igeta. [11] designed an unsupervised stereo matching method for VHR image, validating the feasibility of designing unsupervised methods for VHR images.

Inspired by above previous work, we study unsupervised stereo matching method for VHR image and one potential approach is to generate metric that quantifies disparity error in the absence of disparity ground truth. Multiple methods [6] [12] utilized confidence estimation module to help assess reliability of disparity or generating search range, but those estimations are not correlated to true error. L.Chen [13] successfully combined disparity and uncertainty estimation, achieving improvements in both tasks. H.Shi [12] employed a simple module to generate a binary confidence score for a semi-supervised task. Designing a suitable intermediary metric is essential for refining disparity without ground truth.

In this work, we propose a novel unsupervised stereo matching network based on error prediction for VHR remote sensing images. To overcome the limitation of ground truth, we fit the confidence-aware cascade network (CACN) [14] to unsupervised learning manner. To bridge network confidence with disparity errors, we design a light-weight confidence based error prediction module (CBEM) and demonstrate its cross-domain ability. Leveraging the strong coarse-to-fine ability of multi-scale cascaded core model and error prediction ability of CBEM, our method outperforms the comparison methods in terms of average endpoint error (EPE) and the fraction of erroneous pixels (D1).

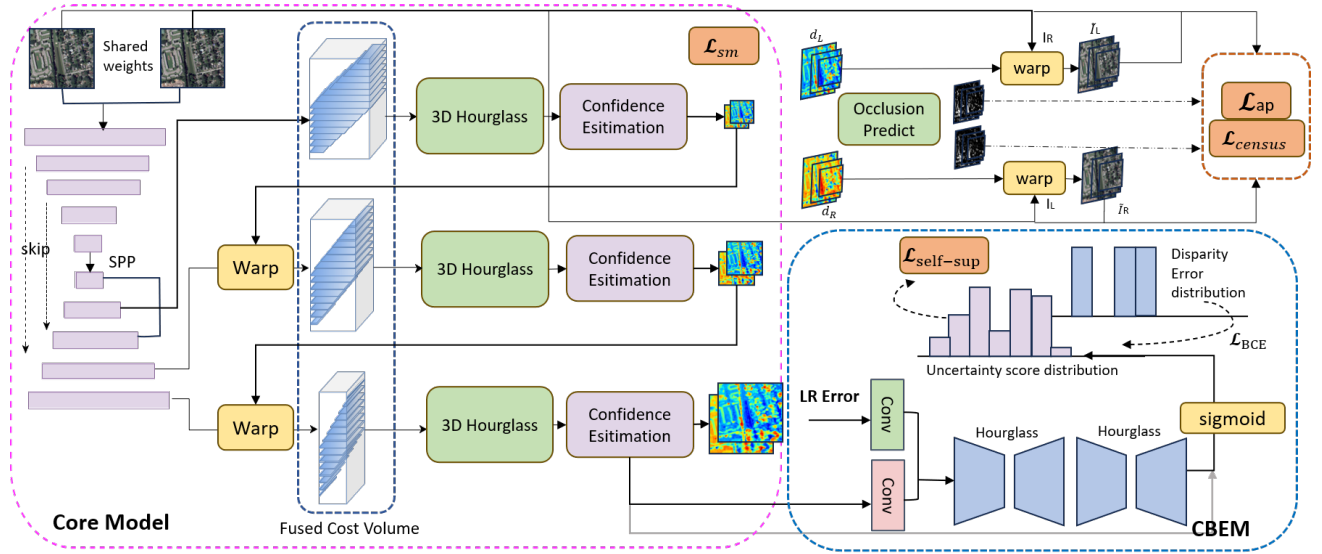


Fig. 1: The framework of proposed method.

2. METHODOLOGY

2.1. The architecture of the proposed network

The complete framework of the proposed network is shown in Fig. 1. The model proposed consists of the core model and confidence based error prediction module (CBEM), while core model is a relatively independent module that predicts disparity following unsupervised learning routine, CBEM predicts uncertainty scores closely associated with disparity errors using confidence outputs of core model. The training process follows a three-step routine: initial training of the core model, subsequent training of the CBEM with the core model fixed, and finally fine-tuning of the core model with CBEM fixed. The last two steps require only a few epochs.

The core model is primarily constructed based on CACN [14]. Below is a brief overview of the structure.

For the feature extraction module, a multi-scale UNet-like network is employed which shares the same weights for both left and right images. Then a combination of concatenated and group-wise correlation modules is utilized to construct cost volume. The initial disparity is generated by softmax operation on cost volume with a range of $[-d_{max}^i, d_{max}^i]$.

Following the coarse-to-fine framework, the search range is estimated using confidence output from the confidence estimation module, calculated as:

$$\begin{aligned} \sigma^i &= \sqrt{\sum_{d^i} (d - \hat{d}^i)^2 \times \text{softmax}(-c_d^i)}, \\ \hat{d}^i &= \sum_{d^i} d \times \text{softmax}(-c_d^i), \end{aligned} \quad (1)$$

where c represents the predicted cost tensor. Then, the disparity range of the next stage can be computed based on the standard deviation σ^i as:

$$\begin{aligned} d_{max}^{i-1} &= \delta(\hat{d}^i + (s^i + 1)\sigma^i + \varepsilon^i), \\ d_{min}^{i-1} &= \delta(\hat{d}^i - (s^i + 1)\sigma^i - \varepsilon^i), \end{aligned} \quad (2)$$

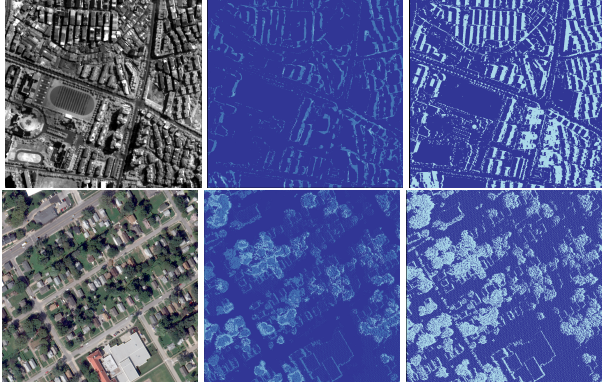
where δ denotes the bilinear upsampling operation. s^i, ε^i are two learnable normalization factors with initial value 0.

The dynamic estimation of the disparity search range based on confidence allows network to reduce computational costs while ensuring accuracy in challenging initial regions. Besides, the confidence output of the core model will be utilized in CBEM module. The multi-scale disparities are optimized by unsupervised loss marked with orange box in Fig.1 and will be discussed in detail in 2.3.

2.2. CBEM: Bridging confidence with disparity error

Motivated by the need to create a module that serves as an intermediary between confidence and true disparity error in order to reduce errors in disparity estimation, we developed the Confidence-Based Error Prediction Module (CBEM). It's not feasible to predict accurate disparity error, otherwise it will be possible to reduce error thoroughly. Thus, we train a simple yet efficient hourglass module to output uncertainty score that aligns with the disparity error distribution. Unlike previous approaches that utilized the disparity to predict uncertainty scores, we used the confidence output from the core model as the input for our module. Although the core model is trained following unsupervised manner, we train CBEM with a few labelled data from WHU-Stereo for only one epoch to gain error prediction ability. Fig. 2 demonstrates the CBEM's stable error prediction capability when directly evaluated on the target US3D dataset. Notably, the CBEM exhibits strong cross-domain generalization ability, as it is less affected by the specific characteristics of original domain, owing to its reliance on confidence rather than disparity as input.

Here, we obtain the final predicted error by jointly encoding LR error and initial uncertainty. LR error is the difference between left image and reconstructed left image using right image and left disparity, as Eq. 3, where \mathcal{W} represents projection operation. The initial uncertainty is generated by core model, thus restricted by its performance, while LR error is not affected by the model. LR error depends on the projection error of left and right images, influenced by local noise and in-



(a) left image (b) uncertainty score (c) disparity error

Fig. 2: CBEM performance on: Top: WHU-Stereo; Bottom: US3D. Warmer colors indicate higher levels of uncertainty or larger disparity errors. The uncertainty score is strongly correlated to disparity error for both WHU-Stereo and US3D.

tensity inconsistency of images, while initial uncertainty does not have this shortcoming. Therefore, these two types of information complement each other well. We firstly encode LR error and initial uncertainty separately by convolution operation. After concatenating them in channel dimension, use two cascaded hourglass modules to learn the residuals of predicted disparity error.

$$E_{LR} = \mathcal{W}(I_r, d_l) - I_l \quad (3)$$

Binary Cross-Entropy loss is adopted to train the CBEM module. Ground truth disparity error above threshold(1.0) is noted as 1, otherwise 0. Data used to train CBEM comes from other datasets with ground truth. Due to its strong cross-domain generalization capability, CBEM still functions well in unsupervised dataset. The formula is as follows.

$$GT_{error} = \begin{cases} 1.0 & |GT_{disparity} - \hat{d}| > 1.0 \\ 0.0 & otherwise \end{cases} \quad (4)$$

$$L_{BCE} = BCE(uscure, GT_{error})$$

2.3. Unsupervised Loss

For the first stage of training, we optimize the core model using unsupervised loss of three scales. The loss function is the same for each scale, denoted L_S . The full loss is the sum of individual scale losses, i.e., $\mathcal{L} = \sum_s \mathcal{L}_s$. The \mathcal{L}_S combines three terms, given as:

$$L_S = \lambda_{ap} \mathcal{L}_{ap} + \lambda_{census} \mathcal{L}_{census} + \lambda_{sm} \mathcal{L}_{sm} \quad (5)$$

$$\mathcal{L}_{ap} = \frac{1}{N} \sum_{i,j} \alpha \frac{1 - SSIM(I_{i,j}^l \odot (1 - O_{i,j}^l), \tilde{I}_{i,j}^l \odot (1 - O_{i,j}^l))}{2} + (1 - \alpha) \left\| I_{i,j}^l \odot (1 - O_{i,j}^l), \tilde{I}_{i,j}^l \odot (1 - O_{i,j}^l) \right\| \quad (6)$$

L_{ap} promotes consistency between left/right image and its reconstructed image in non-occluded areas as Eq. 6, while we

use a simple formulation to detect occluded areas by distance of forward-backward disparities, defined as Eq. 7:

$$|d_i^f(j) + d_i^b(d_i^f(j))|^2 < \tau_i \quad (7)$$

where $d^f(j)$ represents the forward disparity based on left image, $d^b(j)$ represents backward disparity based on right image, $O_{i,j}^l$ is the predicted occlusion map. \odot denotes element-wise multiplication, α is set to 0.85. $\tau_i = [5, 2, 1]$ according to the general pattern of VHR images.

L_{census} is also adopted to reduce reconstruction errors while it has better robustness to various brightness and shadow disturbances in VHR remote sensing images. We utilize Census transform(τ) with a patch size of 7 pixels and Charbonnier penalty function(ρ) to implement L_{census} , Hamming Distance denoted as Γ . The formulation is as follow:

$$\mathcal{L}_{census} = \frac{1}{N} \sum_{i,j} \rho[\Gamma(\tau(I_{i,j}^l), \tau(\tilde{I}_{i,j}^l))] \odot (1 - O_{i,j}^l) \quad (8)$$

L_{sm} is utilized to smooth disparity with L_2 penalty on disparity gradients ∂d and image gradients ∂I , denoted as:

$$\mathcal{L}_{sm} = |\partial_x d_L| e^{-|\partial_x I_L|} + |\partial_y d_L| e^{-|\partial_y I_L|} \quad (9)$$

For the second stage of training, CBEM is fixed to generate a reliable uncertainty score map. As CBEM has gained ability to generate uncertainty score correlated with disparity error, by using fine-scale disparity to supervise coarse-scale disparity in reliable regions, we aim to further refine disparity. Here, we use a mask $M = [uscure < t]$ to exclude poor-performing regions, only focusing on those areas that are good enough. $\mathcal{L}_{self-sup}$ is calculated as follows:

$$\mathcal{L}_{self-sup} = \frac{1}{N} \sum_{i,j} [smooth_{L1}(d_{i,L} - d_{i,j}) \odot M_i] \quad (10)$$

3. EXPERIMENTAL RESULTS

3.1. Dataset

The **SceneFlow dataset** [15] in the finalpass version is used to pretrain our core network, which includes 35,454 positive training and 4370 test images with a resolution of 960×540 , so as the negative ones. **US3D track-2 dataset** [16] of the 2019 Data Fusion Contest is used to evaluate our network, which contains VHR images collected by WorldView-3 between 2014 and 2016 over Jacksonville (JAX) and Omaha (OMA) in the United States. 1712 RGB stereo pairs of JAX are used for training while the remaining 427 pairs are for validation. All 2153 pairs of OMA are used for testing. We also use the with-ground-truth subset of **WHU-Stereo dataset** [17] to validate the cross-domain generalization ability, which contains 1757 GaoFen-7 panchromatic image pairs over Kunming, Qichun, Yingde, Shaoguan, Wuhan and Hengyang in 2020. For training CBEM, we also borrow this dataset to establish relationship between confidence and disparity errors.

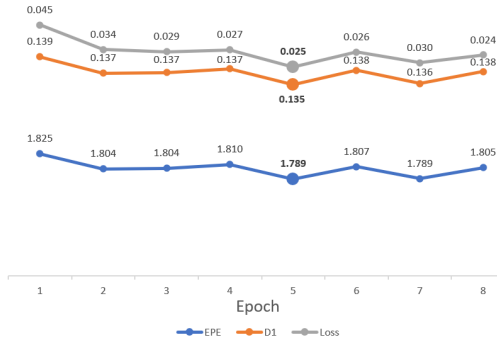


Fig. 3: The validation loss curve.

3.2. Implementation Details

Our network is implemented with PyTorch 1.9.0 and is trained with Adam ($\beta_1 = 0.9, \beta_2 = 0.999$). All input stereo images are randomly cropped to 512×512 for training while 1024×1024 original size is used for testing. We first pre-train our core model on SceneFlow dataset from scratch for 20 epochs with learning rate 0.001 and batch size 8. Then core model is finetuned on US3D dataset in unsupervised manner for 60 epochs with learning rate set to 0.0001. The disparity range is set to $[-128, 128]$. After that, we fix the core model and train CBEM using WHU-Stereo, which only takes 1 epoch with learning rate 0.001 to achieve good error prediction ability. Last step is to fix CBEM and finetune core model with learning rate $1e-5$ for 6 epochs. All experiments are conducted on two NVIDIA Titan-RTX GPUs. To avoid overfitting, we stop training as soon as $\mathcal{L}_{self-sup}$ increases, even though it may drop later. As shown in Fig. 3 on validation set, we plot EPE and D1 curves to demonstrate the need for an immediate stop, Epoch 5 is the best epoch to be adopted.

3.3. Performance

We conducted a comparative analysis between supervised models, namely PSMNet [3] and CACN [14], as well as unsupervised methods including SGBM+WLS [1] and T.Igeta’s model [11], against the proposed method. The evaluation results on US3D dataset are presented in Table. 1 using EPE and D1 as metrics. It is evident that our model outperforms other unsupervised models and gains competitive results compared to supervised models. When comparing with core model, our method improves 11.7 % for EPE and 16.6 % for D1, which proves validity of CBEM.

The core model trained on US3D dataset is directly used to test the WHU-Stereo dataset, revealing the superior cross-domain generalization ability of our proposed unsupervised model, according to Table. 2. As shown in Fig. 4, the proposed method generates disparity with clearer edges of buildings due to smoothing function of \mathcal{L}_{sm} . Furthermore, the proposed method is less prone to missing fuzzy buildings with shadows, owing to the robustness to photometric inconsistency provided by \mathcal{L}_{census} . In the disparities generated by CACN model, building edges usually appear dilated, result-

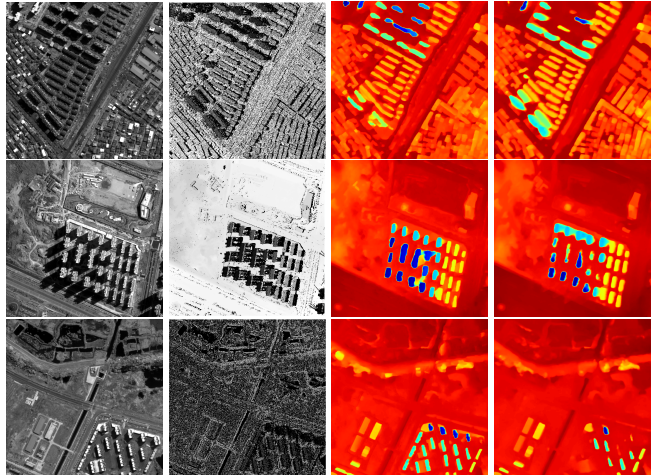


Fig. 4: Disparity estimation on WHU-Stereo. From left to right: left image, GT, proposed, CACN [14].

ing in an overestimation of the building’s size. We have mitigated this issue by incorporating the CBEM module, which reduces predicted disparity error and effectively preserves the precise delineation of building edges.

Table 1: Performance of comparison methods on US3D.

Method	with GT	Deep Learning	EPE	D1(%)
PSMNet [3]	yes	yes	1.48	8.53
CACN [14]	yes	yes	1.47	8.23
SGBM+WLS [18]	no	no	2.56	15.9
T.Igeta et al. [11]	no	yes	2.12	15.3
core model	no	yes	1.96	14.5
Proposed	no	yes	1.73	12.1

Table 2: Performance on WHU-Stereo

Method	with GT	EPE	D1(%)
CACN	yes	3.47	33.5
core model	no	3.11	31.5

4. CONCLUSIONS

In this study, we propose a novel unsupervised stereo matching network based on error prediction for VHR images, which bridges confidence with disparity error, demonstrating robust cross-domain generalizability. For future work, we aim to broaden the scope of the model’s applicability.

5. ACKNOWLEDGEMENT

The authors would like to thank the Johns Hopkins University Applied Physics Laboratory and the IARPA for providing the data used in this study, and the IEEE GRSS Image Analysis and Data Fusion Technical Committee for organizing the Data Fusion Contest. The authors extend their gratitude to Li et al. for supplying the WHU-Stereo dataset utilized in this study. This work was supported by Key Research Program of Frontier Sciences, Chinese Academy of Sciences, under Grant ZDBS-LY-JSC036.

6. REFERENCES

- [1] Heiko Hirschmuller, "Stereo processing by semiglobal matching and mutual information," *IEEE Transactions on Pattern Analysis and Machine Intelligence*, vol. 30, no. 2, pp. 328–341, 2008.
- [2] Alex Kendall, Hayk Martirosyan, Saumitro Dasgupta, Peter Henry, Ryan Kennedy, Abraham Bachrach, and Adam Bry, "End-to-end learning of geometry and context for deep stereo regression," in *2017 IEEE International Conference on Computer Vision (ICCV)*, Oct 2017.
- [3] Jia-Ren Chang and Yong-Sheng Chen, "Pyramid stereo matching network," in *2018 IEEE/CVF Conference on Computer Vision and Pattern Recognition*, Jun 2018.
- [4] Feihu Zhang, Victor Prisacariu, Ruigang Yang, and Philip H.S. Torr, "Ga-net: Guided aggregation net for end-to-end stereo matching," in *2019 IEEE/CVF Conference on Computer Vision and Pattern Recognition (CVPR)*, Jun 2019.
- [5] Xinjing Cheng, Peng Wang, and Ruigang Yang, "Learning depth with convolutional spatial propagation network," *IEEE Transactions on Pattern Analysis and Machine Intelligence*, vol. 42, no. 10, pp. 2361–2379, 2020.
- [6] Zhelun Shen, Yuchao Dai, and Zhibo Rao, "Cfnet: Cascade and fused cost volume for robust stereo matching," in *2021 IEEE/CVF Conference on Computer Vision and Pattern Recognition (CVPR)*, 2021, pp. 13901–13910.
- [7] Rongshu Tao, Yuming Xiang, and Hongjian You, "An edge-sense bidirectional pyramid network for stereo matching of vhr remote sensing images," *Remote Sensing*, vol. 12, no. 24, 2020.
- [8] Simon Meister, Junhwa Hur, and Stefan Roth, "Unflow: Unsupervised learning of optical flow with a bidirectional census loss," *Proceedings of the AAAI Conference on Artificial Intelligence*, Jun 2022.
- [9] Longguang Wang, Yulan Guo, Yingqian Wang, Zhengfa Liang, Zaiping Lin, Jungang Yang, and Wei An, "Parallax attention for unsupervised stereo correspondence learning," *IEEE Transactions on Pattern Analysis and Machine Intelligence*, p. 2108–2125, Apr 2022.
- [10] Sunghun Joung, Seungryong Kim, Kihong Park, and Kwanghoon Sohn, "Unsupervised stereo matching using confidential correspondence consistency," *IEEE Transactions on Intelligent Transportation Systems*, vol. 21, no. 5, pp. 2190–2203, 2020.
- [11] Toshifumi Igeta and Akira Iwasaki, "An unsupervised network for stereo matching of very high resolution satellite imagery," in *IGARSS 2022 - 2022 IEEE International Geoscience and Remote Sensing Symposium*, 2022, pp. 971–974.
- [12] Hongkuan Shi, Zhiwei Wang, Ying Zhou, Dun Li, Xin Yang, and Qiang Li, "Bidirectional semi-supervised dual-branch cnn for robust 3d reconstruction of stereo endoscopic images via adaptive cross and parallel supervisions," *IEEE Transactions on Medical Imaging*, vol. 42, no. 11, pp. 3269–3282, 2023.
- [13] Liyan Chen, Weihang Wang, and Philippos Mordohai, "Learning the distribution of errors in stereo matching for joint disparity and uncertainty estimation," in *IEEE/CVF Conference on Computer Vision and Pattern Recognition, CVPR 2023, Vancouver, BC, Canada, June 17-24, 2023*, 2023, pp. 17235–17244, IEEE.
- [14] Rongshu Tao, Yuming Xiang, and Hongjian You, "A confidence-aware cascade network for multi-scale stereo matching of very-high-resolution remote sensing images," *Remote Sensing*, p. 1667, Mar 2022.
- [15] Nikolaus Mayer, Eddy Ilg, Philip Hausser, Philipp Fischer, Daniel Cremers, Alexey Dosovitskiy, and Thomas Brox, "A large dataset to train convolutional networks for disparity, optical flow, and scene flow estimation," in *2016 IEEE Conference on Computer Vision and Pattern Recognition (CVPR)*, Jun 2016.
- [16] Bertrand Le Saux, Naoto Yokoya, Ronny Hansch, Myron Brown, and Greg Hager, "2019 data fusion contest [technical committees]," *IEEE Geoscience and Remote Sensing Magazine*, p. 103–105, Mar 2019.
- [17] Shenhong Li, Sheng He, San Jiang, Wanshou Jiang, and Lin Zhang, "Whu-stereo: A challenging benchmark for stereo matching of high-resolution satellite images," *IEEE Transactions on Geoscience and Remote Sensing*, vol. 61, pp. 1–14, 2023.
- [18] H. Hirschmuller, "Stereo processing by semiglobal matching and mutual information," *IEEE Transactions on Pattern Analysis and Machine Intelligence*, p. 328–341, Feb 2008.